



CHEMICAL AND LUMINOSITY EVOLUTION, AND COUNTS OF GALAXIES IN A MERGER MODEL *

P. Colin

Instituto de Astronomía
Universidad Nacional Autónoma de México
CP-04510 Mexico, D.F., Mexico

and

D.N. Schramm

University of Chicago, 5640 S. Ellis Ave., Chicago IL 60637

and

NASA/Fermilab Astrophysics Center, Box 500, Batavia, IL 60510

Abstract

A merger model is applied to the chemical and luminosity evolution of galaxies. Two aspects are focused on. The first is the problem of abundance ratios as a function of metallicity. The second is related to the luminosity evolution of galaxies. In relation to the former, we calculate the evolution of several chemical elements exploring a broad space of possible star formation rates, including those derived using phenomenological arguments from a multiple merger galaxy formation scenario. For example, using standard type II supernovae nucleosynthesis scenarios coupled with a reasonable binary model for type Ia supernovae and its consequent nucleosynthetic yields, we can reproduce oxygen abundances. Following the consequent luminosity effects in a straightforward way enables the estimation of the evolution of bolometric luminosity. We have used our recently developed code for photometric evolution of galaxies also to compute preliminarily the number-magnitude relationship, assuming a rather standard picture of galaxy evolution in the B and K bands.

* Submitted to *The Astrophysical Journal*



1. INTRODUCTION

Observational and theoretical evidence permit at least two divergent scenarios for galaxy formation. The first one is some variation of the model of Eggen, Lynden-Bell, & Sandage (1962) in which the disk is formed as a result of the rapid collapse of a gaseous protogalaxy on a timescale of order a few hundred million years (Burkert, Truran, & Hensler 1990). The second one is related to the idea that galaxies are formed by the multiple merger of primordial clouds (Djorgovski 1987, Carlberg 1990b). In this last scenario the formation of the disk could take place after the last major merger occurs (Mathews & Schramm 1990, Mathews et al. 1992) which could enable the disk to be several Gyr younger than the system itself.

Both scenarios take into account the important fact that halo and disk components of the galaxy do have different ages. Based on the luminosity distribution for white dwarf stars, Winget et al. (1987) yield an age of the disk of 9 ± 2 Gyr. Moreover, it is unlikely that the oldest galactic star cluster ages are over 10 billion years (Renzini 1991). Yet we need to have ~ 14 Gyr for the minimum age of the galactic halo (Demarque et al. 1990). While some may relax this bound to 12 or 13 Gyr (Schramm 1989) there are no serious proposals that can reduce the age of the oldest globular cluster to 11 Gyr or less. The single collapse scenario would require a delay of perhaps 4 Gyr between the initial collapse of the galaxy, of which the halo is a relic, and the onset of the star formation in the young thin disk (Burkert et al. 1990). Burkert et al. (1990) attempt to produce a delay due to the cooling time of the halo. In the Mathews & Schramm model (1990), the delay occurs because it is not until after the last merger that the formation of the thin disk can occur.

The merger model is supported by observations (Turscheck 1989) of QSO absorption line systems which show evidence for galaxy-mass multiple cloud systems at high red shift. Furthermore, York et al. (1986) have argued that the QSO absorption lines imply a morphology of galaxies inconsistent with significant disk formation at $z \geq 1$. However some interpret the damped Ly α systems (see Wolfe 1990, for a review) as evidence for early

disks. The merger model is also supported by preliminary observations and theoretical interpretations of emission line objects near QSO absorbers (Yanny & York 1992) which show evidence for clustering of star-forming regions. Thus, a true resolution of the dominance of merger vs. single galaxy evolution must at least await the HST upgrade when the morphology of high z galaxies might be directly observed. It has been noted, however, that quasars and star-burst galaxies themselves may be evidence because they are associated with galaxy collisions (Carlberg 1990a).

There are at least two major motivations for doing galaxy counts versus magnitude, redshift, or color. The first is to search for some cosmological effect: to find the cosmological parameters, the deceleration q_0 parameter (or density Ω_0) and the cosmological constant Λ_0 , respectively. The second is to investigate galaxy evolution through the luminosity term. Obviously, unless one understands the second, the first is unreliable. It is for this reason that this paper will examine the merger luminosity evolution so that we can eventually discuss constraints on Ω_0 and Λ_0 from merger models in contrast to arguments using "standard" luminosity evolution (Yoshii & Takahara 1988; Fukugita et al. 1990; Guiderdoni & Rocca-Volmerange 1990; Cowie et al. 1992; Koo & Kron 1992; Carlberg & Charlot 1992).

For some time it has been recognized that the star formation rate (SFR) plays a central role in models of the chemical evolution of galaxies (see, for instance, Tinsley 1980). So far, most calculations have taken into account only the chemical evolution of the disk. They assume that the disk is already formed and use an SFR as a continuous process of star generation. The analytic behavior of the SFR covers a wide spectrum of possibilities, from an exponential dependence on galaxy age (Miller & Scalo 1979) up to power law gas density dependence (Schmidt 1963; Matteucci & Greggio 1986). In the model we are considering, star formation is also associated with the mergers. Actually, galaxies in which the star formation occurs in a small number of bursts evolve their abundances in a manner different from models of galaxies with continuous star formation. Gilmore and

Wyse (1991) show that an underabundance of oxygen observed in the Large Magellanic Cloud may be explained by a series of bursts of star formation.

It is well known that there is a characteristic initial plateau in the $[\text{Fe}/\text{O}]$ vs. $[\text{Fe}/\text{H}]$ plot observed in the halo oxygen abundances (Barbuy 1988; Smecker & Wyse 1992 and references therein). It is often explained as being due to the different timescales in the type II and Ia supernovae (e.g., Smecker & Wyse 1992). Oxygen is created almost exclusively in high mass stars and ejected in the type II supernovae event, whereas iron is heavily created by the much longer-lived type Ia supernovae. Once the type Ia turns on, the $[\text{Fe}/\text{O}]$ commences to increase. Here we note that similar behavior for $[\text{Fe}/\text{O}]$ can be sustained if there exist a particular exponential behavior of the SFR, like the one suggested by the old Mathews-Schramm star formation rate (Mathews & Schramm 1990). As we will see below, it is the old Mathews-Schramm SFR (hereafter called OMS) of the various recent merger inspired SFR's proposals, which predicts a plateau in the iron to oxygen ratio. Indeed, a plateau at much lower metallicity would always be observed, no matter what the SFR is, as a result only of the type Ia effect. That a particular SFR could produce a flat behavior in the oxygen abundances at low halo metallicity and thereby explain the full oxygen abundance trend had not been noticed before (at least not explicitly stated).

In this paper a merger model for galaxy formation has been explored using star formation rates which are supported by phenomenological arguments. We note that the star formation scenario we are treating is a more complete history of the galaxy, including the formation of the halo, than that attempted by most traditional chemical evolution models. We show that one SFR model we use reproduces the age-metallicity relationship and the oxygen abundances to a reasonable accuracy. The model leads to a luminosity evolution which may explain the recent observations of the galaxy number counts in the blue and infrared color bands (Lilly et al. 1991; Cowie et al. 1992).

2. A CHEMICAL EVOLUTION MODEL

Let us begin by describing our numerical model of chemical evolution, noting the necessary ingredients included in any model of chemical evolution.

2.1 Initial Conditions and Input Parameters

Initial Conditions. We are using a complete disk-halo model. We are not invoking infall of primordial or enriched gas as many chemical evolution models do. That is, we are assuming the galaxy started as a cloud or more precisely clouds of primordial gas, whose total mass value is the actual mass of the present galaxy, without ejecting or accreting other unaccounted material in its further development.

Stellar Birthrate Function. It is known that the stellar birthrate should be a function of both time and stellar mass. However, in the absence of a complete understanding of the star formation process and for reasons of simplicity, the stellar birthrate $B(m,t)$ is often separated into two independent functions:

$$B(m,t) = \psi(t)\phi(m), \quad (1)$$

where $\psi(t)$ is the star formation rate (SFR) in units of Gyr^{-1} and $\phi(m)$ the initial mass function (IMF) in $M_{\odot}^{-1}pc^{-2}$. Here we will assume that the IMF is independent of time and space. Certainly this would not be true, for example, if the IMF were a function of metallicity. For example, there are authors (see, for instance, Schmidt 1963) who have used this condition in order to explain the G-dwarf problem (scarcity of metal-poor stars). However, since we do not have, at present, a clear idea of how the IMF varies, out of ignorance, the assumption of an IMF constant in space and time will be used in this preliminary exploration.

For simplicity we have used a lower mass limit of the IMF at $0.1 M_{\odot}$, thus eliminating the possibility of having brown dwarfs (see below). Although this will not play any role in chemical evolution, it could have appreciable consequences on the dynamics of the galaxy

and the nature of dark halos. In future papers a variable IMF will be explored along with the role of the low mass cutoff.

Stellar Nucleosynthesis, Supernovae Rates, and Stellar Lifetimes. Let us note that stars with different masses and chemical compositions have different nucleosynthetic histories: thus they contribute in different ways to galactic chemical enrichment. For instance, stars with masses less than $\simeq 0.8M_{\odot}$ do not contribute to galactic chemical enrichment because their lifetime is greater than the age of the Universe, although they live long enough that they serve as a sink for material. On the other hand, stars with masses greater than $\simeq 9M_{\odot}$ are responsible for the bulk of heavy elements such as O, Ne, Mg, Si etc. and probably r-process elements (Arnett & Schramm 1973; Arnett 1978; Woosley & Weaver 1986). They also contribute to ^{12}C and ^{56}Fe (Arnett, Schramm, & Truran 1989). These massive stars eject the newly synthesized elements through supernovae explosions of type II and Ib. For the case of supernovae type Ia, we have utilized the binary model of Greggio & Renzini (1983). The important point here is that the explosion is delayed until the secondary component fills its Roche Lobe and begins to transfer matter onto the degenerate companion. The delay time will depend on whether the primary star is a C/O-White Dwarf or a He-White Dwarf precursor, being $\sim 10^7$ or $\sim 10^9$ yr, respectively.

2.2 Numerical Model

Our numerical model of the chemical evolution is based on the following two equations (see Tinsley 1980, for a review):

$$dm_g/dt = -B(t) + P(t) + f_I(t), \quad (2)$$

$$dm_i/dt = P_i(t) + E_i(t) - X_i(0)f_I - Bm_i(t)/m_g(t). \quad (3)$$

In equation (2), m_g denotes the gas density in units of $M_{\odot} \text{ pc}^{-2}$. B represents the rate at which material is lost from interstellar medium (ISM) to stars:

$$B(t) = \int_{m_{low}}^{m_{high}} m \phi(m) \psi(t) dm. \quad (4)$$

$P(t)$ the rate at which gas is returned to the ISM by dying stars:

$$P(t) = \int_{m(t)}^{m_{high}} (m - m_r) \phi(m) \psi(t - \tau(m)) dm. \quad (5)$$

and finally f_I is any net infall of gas from outside the system which in our case is set to zero. In equation (3), m_i represents the mass of the element i per unit area in the ISM, P_i the rate at which the element i is produced and ejected into the ISM, E_i the rate at which stars return whatever is left of their original abundance:

$$E_i = \int_{m(t)}^{m_{high}} (m - m_r) \phi(m) \psi(t - \tau(m)) \frac{m_i(t - \tau(m))}{m_g(t - \tau(m))} A_i(m) dm. \quad (6)$$

and finally $X_i(0)$ the primordial mass fraction of species i .

Furthermore, m_r is the mass that is left once the star died, $\tau(m)$ is the lifetime of a star, $m_i(m)$ is the mass of a star that is ejected as newly synthesized element i , and $A_i(m)$ is the factor by which element i is depleted in a star of mass m . For example, for ^2D and ^7Li and others light elements, A_i can be chosen to be zero to a very good approximation (Brown 1992); moreover, for iron and oxygen these terms will be unity.

2.3 Star Formation Rates

As we mentioned before, the choice of the star formation rate is usually the most sensitive parameter for models of chemical evolution. For this calculation we have chosen various star formation rates. These are explicitly written below. Our SFR's satisfy the two major constraints: $\langle \psi(t) \rangle / \psi(T_g) \leq 2.5$ (Twarog 1980) and the continuity constraint, $0.18 \leq T_g \psi(T_g) \leq 2.5$ (Scalo 1986), where T_g represents the age of the galaxy. A value of 15 Gyr for T_g will be assumed although the results can all be easily scaled up or down by several Gyr.

The most straightforward possible choices for an SFR are (Brown 1992): a constant SFR,

$$\psi(t) = 1/T_g. \quad (7)$$

a maximally exponentially increasing SFR.

$$\psi(t) = \frac{0.41e^{(1.6t/T_g)}}{T_g}. \quad (8)$$

and a maximally exponentially decreasing SFR.

$$\psi(t) = \frac{2.6e^{(-2.4t/T_g)}}{T_g}. \quad (9)$$

We will also be using SFR's that might simulate the multiple merger SFR, the old Mathews-Schramm SFR (OMS):

$$\psi(t) = \begin{cases} A[re^{-t/t_0} - 1]e^{5t/3t_0} & t/t_0 \leq \ln r \\ B & t/t_0 \geq \ln r \end{cases}. \quad (10)$$

where it can be noted that $\psi(t) \propto e^{2t/3t_0}$ for $t/t_0 \ll \ln r$, and the new Mathews-Schramm SFR (Mathews et al. 1992) (NMS):

$$\psi(t) = a + b\delta(t - t_1)e^{-(t-t_1)/\tau_1} + c\delta(t - t_2)e^{-(t-t_2)/\tau_2}. \quad (11)$$

In both expressions the parameters have to do with the characteristics that govern the behavior of the model which are: (i) a first burst followed by a more quiet star formation rate due to sporadic mergers and intrinsic quiescent star formation in the colliding clouds and (ii) a second burst as a result of the last major merger followed by the star formation rate in the disk.

The differences between OMS and NMS are: (1) there is no first burst in OMS; i.e. the second term in eq. (11) does not exist in OMS at all, (ii) the constant term due to the assumed quiescent SFR in the clouds, the first term in NMS, does not appear in OMS, and (iii) the assumed SFR in the disk is different—whereas in OMS it is constant, in NMS it is exponentially decreasing. We will see later how these characteristics play a primary role in determining the behavior of the abundance ratios vs. metallicity.

We mentioned above that by taking the lower mass limit, m_{low} , of the IMF as $0.1M_{\odot}$, we eliminate the possibility of having brown dwarfs. At the present time there is no observational evidence nor strong theoretical arguments about the lower mass cutoff of the IMF.

Including the deuterium burning limit (Adams & Walker 1989) or the evaporation lower limit (Rújula, Jetzer, & Massó 1991) on m_{low} , it still allows a broad range of possibilities so that brown dwarfs remain a viable candidate for dark galactic halos. In a subsequent paper we will explore such possibilities; however, in this paper we will focus on the chemical evolution where these low mass objects have little effect so we can utilize a high m_{low} .

The upper limit, m_{high} , is related to the question: how large can nature make a star? Fortunately, this uncertainty also does not have much influence on models of chemical evolution because at the high end the standard IMF is negligibly small. For definiteness in our model we have taken $m_{low} = 0.1 M_{\odot}$ and $m_{high} = 62 M_{\odot}$.

The next parameter to consider is the shape of the IMF. We derived the IMF from the mass function, $\xi(m)$ of Rana (1987) and our star formation rate.

$$\phi(m) = \xi(m) / \int_{T_g - \tau(m)}^{T_g} \psi(t) dt. \quad (12)$$

To solve eq. (1) it remains only to specify the remnant mass. We assume the remnant mass from Iben & Renzini (1983)

$$m_r(m) = \begin{cases} m & m \leq 0.45 \\ 0.15m + 0.38 & 0.45 < m < 6.8 \\ 1.4 & m \geq 6.8 \end{cases} . \quad (13)$$

Under the condition $m_g(T_g) = 13 \pm 3 M_{\odot} pc^{-2}$ (Kulkarni & Heiles 1987), values of the total galactic disk surface density $m_g(0)$, reasonably close to the observed value $M_{tot} = 46 \pm 9 M_{\odot} pc^{-2}$, are produced (Gilmore, Wyse, & Kuijken 1989).

2.4 Supernovae Rates

Let us now discuss P_i , the rate at which the element i is produced and ejected into the interstellar medium. Generally speaking, there are three sites of element production: 1) big-bang nucleosynthesis (e.g., Olive et al. 1989), 2) the interstellar medium (via cosmic-ray interactions; Walker, Mathews, & Viola 1985), and 3) stars (e.g., Burbidge et al. 1957).

Except for ^1H , ^4He , ^2D , ^3He and some ^7Li which are produced in the big bang, the other nucleosynthetic products relate in one way or another to the formation of stars. In this paper we will concentrate just on those elements whose primary production comes from supernovae events. For the sake of illustration let us take oxygen relative to iron. It is well known that the ratio $[\text{Fe}/\text{O}]$ varies as a function of metallicity ($[\text{Fe}/\text{H}]$) (see, for example, Wheeler, Sneden, & Truran 1989). This underabundance of iron in stars of low metallicity can be explained by differences between the lifetime of oxygen (mainly type II supernovae) and iron producers (partly type Ia supernovae).

For the calculation of P_i we have assumed the binary model of supernovae of type Ia. According to Greggio & Renzini (1983), the supernovae rate for Ia's (SN Ia) is given by

$$R_{SNIa} = r_{SNIa} \int_{m_{inf}}^{m_{max}} \phi(m_B) \int_{\mu_{inf}}^{0.5} f(\mu) \psi(t - \tau(\mu m_B)) d\mu dm_B, \quad (14)$$

where m_B is the mass of the binary system, μ is the mass fraction of the secondary star m_2/m_B , and $f(\mu)$ the distribution function of μ :

$$f(\mu) = 2^{1+\gamma}(1 + \gamma)\mu^\gamma, \quad (15)$$

and we have used $\gamma = 2$ as adopted by Matteucci & Greggio (1986).

With m_{min} and m_{max} we denote the minimum and the maximum binary mass to produce a SN Ia event. Adopting the C-deflagration model (Nomoto, Thielemann, & Wheeler 1984) we have considered carbon and oxygen white dwarfs as SNIa progenitors, which implies $m_{max} = 16M_\odot$. For m_{min} we have used $3 M_\odot$. The expressions of m_{inf} and μ_{inf} are given by:

$$m_{inf} = \max[2m_2(t), m_{min}], \quad (16)$$

and

$$\mu_{inf} = \max[m_2(t)/m_B, (m_B - 0.5m_{max})/m_B]. \quad (17)$$

On the other hand, the oxygen producing types Ib and II supernovae are probably the result of high-mass star evolution. Therefore, it is natural to assume that the rates are

given by:

$$R_{(SNII \text{ and } SNIb)} \propto \int_{m_{low}}^{m_{high}} o(m) \nu(t - \tau(m)) dm, \quad (18)$$

where the integration limits are taken from 9 to 30 M_{\odot} for SNII, and 30 to 62 M_{\odot} for SNIb.

Going back to P_i , we now have the necessary information to give an explicit expression, namely:

$$P_i(t) = m_{i, Ia} R_{SNIa}(t) + m_{i, Ib} R_{SNIb}(t) + m_{i, II} R_{SNII}(t), \quad (19)$$

where $m_{i, I's}$ are the masses of the element i ejected per supernovae of each type. We assume $m_{i, Ia}$ from the W7 model of Nomoto, Thielemann, & Wheeler (1984), $m_{Fe, Ib}$ from Cahen, Schaeffer, & Casse (1985), and for $m_{Fe, II}$ the value of the SN 1987A $\sim 0.07 M_{\odot}$. We do certainly expect stellar yields to vary with mass (Woosley & Weaver 1986; Arnett, Schramm, & Truran 1989), but we do not know the details. Therefore, for simplicity we have used constant values for the yields over each type. Moreover, the overall rate and yields are normalized to give the presently observed ratios, $R_{SNIb}/R_{SNIa} = 1$ and $R_{SNII}/R_{SNIa} = 3.3$ (Evans, van den Bergh, & McClure 1989) and solar abundances (Cameron 1982) 4.6 Gyr ago.

2.5 Results

The calculated age-metallicity relationship compared with observations (Twarog 1980; Carlberg et al. 1985) is plotted in figure 2 (a-b) for the distinct star formation rates. Taking into account the uncertainties on deriving the age of these stars, the results are in reasonable agreement with observations, except, perhaps, for the so-called hiatus star formation rate (HIATUS) and NMS. Yet, inside the parameter space, we find some values of the parameters which give better fits; however, these values exacerbate the [Fe/O] vs. [O/H] problem and contradict other restrictions (Mathews 1992), clearly illustrating that the models, to date, are still not complete (or some of the observations are in error).

Following Wheeler et al. (1989), we have plotted [Fe/O] vs. [O/H] (fig. 3 a-b),

using $[O/H]$ as a better indicator of metallicity, since most of the oxygen is coming from type II supernovae events, for the different types of star formation rate and two different prescriptions of the yields. Data taken from Nissen et al. (1985) and Barbuy (1988) are well fitted by the OMS star formation rate where contributions of SNIb and SNII for iron are less important. Whereas an iron underabundance relative to oxygen is seen at low metallicity for all the star formation rates (fig. 3a) and it is explained here due to the difference in the timescale between the type II and type Ia supernovae, the plateau is characteristic only of OMS. The flat part is sustained during a few Gyr after the ignition of the type Ia supernovae due to the particular exponential increasing behavior of OMS (fig. 3b). In this case, the solar abundances $[Fe/O] = 0.0$ are delayed until the last major merger has happened.

What is really making the difference between the two merger-inspired, model-dependent star formation rates, OMS and NMS, is the first stellar burst omitted in OMS. The low-mass stars born in the burst will increase the iron to oxygen ratio, through the type Ia supernovae, during the hiatus time producing that jump which is seen in NMS and HIATUS (see fig. 3a). There are SFR's, e.g., a constant SFR, which have no first burst and still have an increasing trend in $[Fe/O]$, however. Thus it is necessary to have this exponentially increasing behavior with the right timescale in order to produce a flat behavior in the iron to oxygen ratio. It is clear that when this exponential behavior disappears then the type Ia effect takes over and a rapid increasing in $[Fe/O]$ is expected to occur (see fig. 3b and the solid line in fig. 3a).

We have also computed the abundances of several others oxygen family elements. In figure 4a-c we have plotted the Mg, Si, and Ti abundances for the iron yield prescription which fits the oxygen abundance.

Within the framework of our simple model of chemical evolution, the ratio $R = (m_{i,Ia}/m_{i,II})/(m_{Fe,Ia}/m_{Fe,II})$ is a primary quantity for the calculated abundances. When an element has a value of R lower than 1, it will be overabundant; conversely, if it has R

greater than 1, it will be underabundant. We have calculated R for various elements and found that O, Na, Mg, and Ti behave similarly; i.e., they are all overabundant. To a lesser extent we have also found Si and S to be overabundant; however, in the case of Ca, R is greater than 1. This pattern comes, on the one hand, from the constraint we have given to the yields, namely, they have to fit the solar abundances; and, on the other hand, from the adopted prescription of Nomoto et al. (1984) for $R_{SN Ia}$ yields. Regarding the problem of the underabundance of the Ca, a possible solution would be to decrease the theoretical yield of calcium from type Ia supernovae.

3. THE NUMBER-COUNT RELATIONSHIP

Following Sandage (1988), in order to find the number of galaxies versus apparent magnitude in a certain band characterized by λ , m_λ , the following necessary ingredients are required: (i) a cosmological model for the volume enclosed in redshift distance z , $V(z, q_0)$, (ii) the luminosity function of galaxies of different types, $\Phi^i(M_\lambda)$, (iii) the density of galaxies per comoving volume as a function of z , $D^i(z)$, and finally, (iv) a redshift-magnitude relation.

The galaxy count data are obtained by counting up all galaxies on a finite area of the sky. If $n(m_\lambda, z)dm_\lambda dz$ represents the number of galaxies between m_λ and $m_\lambda + dm_\lambda$ and between z and $z + dz$, then we have

$$n(m_\lambda, z) = \frac{\omega}{4\pi} \frac{dV}{dz} \sum_{i=1}^n D^i(z) \Phi^i(M_\lambda), \quad (20)$$

where ω is the angular area in units of steradians over which the galaxies are counted and n is the number of galaxy types. The apparent magnitude m_λ is related to the absolute magnitude M_λ through.

$$m_\lambda(z) = M_\lambda + K_\lambda(z) + E_\lambda(z) + 5 \log(d_L(z)/10pc). \quad (21)$$

The K_λ and E_λ terms represent the correction factor for the frequency shift due to the change in redshift and the luminosity evolution of a galaxy, respectively. Finally, we have defined d_L as the luminosity distance (see, for instance, Weinberg 1972).

The differential number count is given by integrating $n(m_\lambda, z)$ with respect to z from $z = 0$ to $z = z_f$, where z_f denotes the redshift of galaxy formation:

$$n(m_\lambda) = \int_0^{z_f} n(m_\lambda, z) dz. \quad (22)$$

Here we have assumed a value of 3 for z_f . The sensitivity to this assumption will be explored in a subsequent paper.

3.1 The Evolution of the Bolometric Luminosity

To find the integrated luminosity of the stellar system we will divide the stars in two classes: Main Sequence (ms) and Post-Main Sequence (pms) or giants stars. We will not consider white dwarfs because their contribution to the total luminosity is negligible. Following Tinsley (1980) we have that the dwarf luminosity, l_d , is given by:

$$l_d(t) = \int_{m_{low}}^{m_{high}} n_d(m, t) l_d(m) dm, \quad (23)$$

where $n_d(m, t)$ is the number density of ms stars per unit area at time t :

$$n_d(m, t) = \begin{cases} \int_{t-\tau(m)}^t \phi(m) \psi(t') dt' & \tau(m) < t \\ \int_0^t \phi(m) \psi(t') dt' & \tau(m) \geq t, \end{cases} \quad (24)$$

and $l_d(m)$ is the mass-luminosity relation for ms stars. Again the integration limits are $m_{low} = 0.1$ and $m_{high} = 62$.

The Post-Main Sequence or giants luminosity, l_g , is found using the Fuel Consumption Theorem (Renzini & Buzzoni 1986).

$$\begin{aligned} l_g(t) &= \int_{m_{low}}^{m_{high}} l_g(m) n_g(m, t) dm \\ &\approx 97.5 \times 0.5 \int_{m_{low}}^{m_{high}} n_g(m, t) / \tau_g(m) dm. \end{aligned} \quad (25)$$

where $n_g(m, t)$ is the number density of giants per unit area at time t :

$$n_g(m, t) = \int_{t-(\tau(m)+\tau_g(m))}^{t-\tau(m)} \phi(m)\psi(t')dt'. \quad (26)$$

and $\tau_g(m)$ is the time that a star of mass m spends after leaving the ms stage until it becomes a white dwarf. It is roughly,

$$\tau_g(m) \simeq 1.66m^{-2.72}Gyr. \quad (27)$$

In this case the value of the inferior integration limit in eq. (25) is $m_{low} \sim 1M_{\odot}$ and the superior is still $62 M_{\odot}$.

Once we have obtained the luminosity evolution and assuming a value for q_0 ($q_0 = \Omega_0/2$ for $\Lambda_0 = 0$) and h_{50} , where h_{50} is the Hubble constant in units of $50 km sec^{-1} Mpc^{-1}$, (here, we take $q_0 = 1/2$ and $h_{50} = 1$) the expression for $E_{Bol}(z)$ is given by,

$$E_{Bol}(z) = \Delta M_{Bol}(z) = -2.5 \log[L(z)/L(0)]. \quad (28)$$

In figure (5) (a-b) we show ΔM_{Bol} as a function of redshift and age for the different SFRs.

We have followed Yoshii & Takahara (1988) to compute the number count of galaxies and used a Schechter fit to the luminosity function independent of type. To describe the spectrophotometric properties of evolving galaxies, we compute five models with exponentially-decreasing star formation rates with star formation timescales of 0.5, 3.0, 5.0, 9 and ∞ roughly corresponding to E/SO, Sa, Sb, Sc, and Sd/Im galaxies (Yoshii & Takahara 1988; Charlot & Bruzual 1991). In figure 6a-b the number count of galaxies is plotted in the blue B_J , and in the near infrared K band for $z_f = 3.0$ and $\Omega_0 = 1.0$, the data points are from Maddox et al. (1990), Metcalfe et al. (1991), and Lilly et al. (1991) (these latter kindly made available to us by R. Kron) for the B_J band and from figure 5 (panel II) of Cowie et al. (1992) for the K band. It is seen, as many authors have emphasized, how the $(\Omega_0, \Lambda_0) = (1, 0)$ cosmological model with a standard picture of galaxy evolution does not reproduce the number-magnitude observations when we simultaneously

look at two different bands. As we mentioned before, a consistent number and luminosity evolution may explain such discrepancies (Carlberg & Charlot 1992) in a merger model. We will explore this in a subsequent paper. In particular, we will use the Mathews and Schramm SFR's and our photometric evolution of galaxies code to model the magnitude and color evolution of galaxies. We will estimate how the density of galaxies per comoving volume may have evolved. Once we have quantified the luminosity and density evolution effects, we will be able to see how the number of galaxies vs. magnitude, redshift, and color are affected.

4. CONCLUSIONS

We have utilized different prescriptions for the star formation rate. In particular, we have used a phenomenological merger model for the galaxy formation to evaluate abundance ratios as a function of metallicity. We reproduce relatively well the O, Mg, Si, and Ti abundances and the age-metallicity relation for the old Mathews-Schramm SFR. Although there are still some elements whose abundance ratios are not yet well fit, we feel the success with the dominant nuclei encourages us to proceed to more complex tests for this simplified model.

We have also calculated the bolometric luminosity evolution of galaxies assuming this picture. The model along with our photometric evolution of galaxies code may account for the different types of galaxies by varying the parameters of the SFR. With a suitable number density evolution the model might explain recent observations of faint galaxy number counts. Subsequent papers will explore the cosmological and extragalactic implications in greater detail as well as the sensitivity to IMF assumptions. This present paper has sufficiently demonstrated the basic framework of a merger inspired SFR on abundance evolution to justify the increased parameter space search that these additions will require.

ACKNOWLEDGEMENTS

We would like to thank Grant Mathews for inspiration on many aspects of the problem. We would also like to thank Larry Brown and Jim Truran for their useful discussions on the chemical evolution problem. This work was supported in part by Universidad Nacional Autonoma de Mexico and by NSF grant AST90-22629. NASA grant NAGW 1321 and DOE grant DE-FG02-91 ER40606 at the University of Chicago, and by the DOE and by NASA through grant 2381 at Fermilab.

REFERENCES

- Adams, F., & Walker, T.P. 1990. *ApJ*, 359, 57
- Arnett, W.D. 1978. *ApJ*, 219, 1008
- Arnett, W.D., & Schramm, D.N. 1973. *ApJ*, 184, L47
- Arnett, W.D., Schramm, D.N., & Truran, J.W. 1989. *ApJ*, 339, L25
- Barbuy, B. 1988. *A&A*, 191, 121
- Brown, L. 1992. *ApJ*, 389, 251
- Burbidge, E.M., Burbidge, G., Fowler, W., & Hoyle, F. 1957. *Rev. Mod. Phys.*, 29, 547
- Burkert, A., Truran, W.J., & Hensler, G. 1990. preprint
- Cahen, S., Schaeffer, R., & Casse, M. 1985. in *Nucleosynthesis and Its Implications on Nuclear and Particle Physics*, ed. J. Audouze & N. Mathieu (Dordrecht: Reidel), 243
- Cameron, A.G.W. 1982, in *Essays in Nuclear Astrophysics*, ed. C. Barnes, D. Clayton, & D.N. Schramm (Cambridge: Cambridge Univ. Press), 23
- Carlberg, R.G. 1990a. *ApJ*, 350, 505
- Carlberg, R.G. 1990b. *ApJ*, 359, L1
- Carlberg, R.G., Dawson, P.C., Hsu, T., & Vandenberg, D.A. 1985, *ApJ*, 294, 674
- Carlberg, R.G., & Charlot, S. 1992, *ApJ*, in press
- Charlot, S., & Bruzual, A.G. 1991, *ApJ*, 367, 126
- Cowie, L.L., Gardner, J.P., Hu, E.M., Wainscoat, R.J., & Hodapp, K.W. 1992. preprint
- Demarque, P., Deliyannis, C.P. & Sarajedini, A. 1990, Yale University preprint
- De Rújula, A., Jetzer, P., & Massó, E. 1991, CERN preprint TH.5787/91
- Djorgovski, S. 1987. in *Starbursts and Galaxy Evolution*, ed. T.X. Thuan, T. Montmerle, & J. Tran Thanh Van (Singapore: Editions. Frontieres), 401

- Eggen, O.J., Lynden-Bell, D., & Sandage, A.R. 1962. *ApJ*, 136, 748
- Evans, R., van der Bergh, S., & McClure, R.D. 1989. *ApJ*, 345, 752
- Fukujita, M., Takahara, F., Yamashita, K., & Yoshii, Y. 1990. *ApJ*, 361, L1
- Gilmore, G., Wyse, R.F.G., & Kuijken, K. 1989. *ARA&A*, 27, 555
- Gilmore, G., & Wyse, R.F.G. 1991. *ApJ*, 367, L55
- Gratton, R.G., & Sneden, C. 1987. *A&A*, 173, 179
- Gratton, R.G., & Sneden, C. 1988. *A&A*, 204, 193
- Greggio, L., & Renzini, A. 1983. *A&A*, 118, 217
- Guiderdoni, B., & Rocca-Volmerange, B. 1990. *A&A*, 227, 362
- Hartmann, K., & Gehren, T. 1988. *A&A*, 199, 269
- Koo, D.C., & Kron, R.G. 1992. *ARA&A*, in press
- Kulkarni, S.R., & Heiles, C. 1987. in *Interstellar processes*, ed. J. Hollenbach & H. A. Thronson (Dordrecht: Reidel), 87
- Lilly, S.J., Cowie, L.L., & Gardner, J.P., 1991. *ApJ*, 369, 79
- Maddox, S.J., Sutherland, W.J., Efsthathiou, G., Loveday, J., & Peterson, B.A. 1990. *MNRAS*, 247, 1P
- Magain, P. 1989. *A&A*, 209, 211
- Mathews, G.J. 1992. private communication
- Mathews, G.J., & Schramm, D.N. 1990. LLNL preprint UCRL-JC-106176
- Mathews, G.J., Bazan, G., Cowan, J., & Schramm, D.N. 1992. *Phys. Rep.*, in press
- Matteucci, F., & Greggio, L. 1986. *A&A*, 154, 279
- Metcalf, N., Shanks, T., Fong, R., & Jones, L.R. 1991. *MNRAS*, 249, 498
- Miller, G.E., & Scalo, J.M. 1979. *ApJS*, 41, 513

- Nissen, P.E., Edvardsson, B., & Gustafsson, B., 1985, in *Production and Distribution of C, N, O Elements*, ed. E.J. Danziger, F. Matteucci, & K. Kj ar (Garching: European Southern Observatory), 131
- Nomoto, K., Thielemann, F.K., & Wheeler, J.C. 1984, *ApJ*, 286, 644
- Olive, K., Schramm, D.N., Steigman, G., & Walker, T. 1989, Fermilab preprint 89/262-A
- Rana, N.C. 1987, *A&A*, 184, 104
- Renzini, A. 1991, Universita di Bologna preprint BAP 02-1991-007-DDA
- Renzini, A., & Buzzoni, A. 1986, in *Spectral Evolution of Galaxies*, ed. C. Chiosi & A. Renzini (Dordrecht: Reidel), 195
- Sandage, A. 1988, *ARA&A*, 26, 561
- Scalo, J.M. 1986, in *FunCosP*, 11, 1
- Schmidt, M. 1963, *ApJ*, 137, 758
- Schramm, D.N. 1990, in *Astrophysical Ages and Dating methods*, ed. E. Vangioni-Flam et al. (Gif-sur-Yvette, France: Editions Frontieres), 365
- Smecker, T.A., & Wyse, R.F.G. 1992, *AJ*, in press
- Tinsley, B.M. 1980, *FunCosP*, 5, 287
- Turscheck, et al. 1989, *ApJ*, 344, 567
- Twarog, B.A. 1980, *ApJ*, 242, 242
- Walker, T.P., Mathews, G.J., & Viola, V.E. 1985, *ApJ*, 299, 745
- Weinberg, S. 1972, in *Gravitation and Cosmology* (New York: Wiley)
- Wheeler, J.C., Sneden, C., & Truran, J.W. 1989, *ARA&A*, 27, 279
- Winget, D.E., et al. 1987, *ApJ*, 315, L77
- Wolfe, A.M. 1990, in *The Interstellar Medium in Galaxies*, ed. H.A. Thronson & J.M. Shull (Dordrecht: Kluwer), 387

- Woosley, S.E., & Weaver, T.A. 1986. in *Nucleosynthesis and Its Implications for Nuclear and Particle Physics*, ed. J. Audouze & N. Mathieu (Dordrecht: Reidel), 145
- Yanny, B. & York, D.G. 1992. *ApJ*, 391, 569
- York, D.G., Dopita, M., Green, R., & Bechtold, J. 1986. *ApJ*, 311, 610
- Yoshii, Y., & Takahara, F. 1988. *ApJ*, 326, 1

FIGURE CAPTIONS

Fig. 1 Here we have plotted the six different star formation rates. The solid line is for the old Mathews and Schramm SFR (OMS). The dotted, short-dashed, long-dashed, and dot-long-dashed for the constant, exponential increasing, exponential decreasing, and the new Mathews and Schramm SFR (NMS) respectively. The behavior of the age-metallicity for the hiatus SFR (HIATUS) is represented for the dot-short-dashed.

Fig. 2a-b The age-metallicity relationship as predicted by the model for the six distinct star formation rates. As in the figure 1, the solid line is for OMS, the dotted line for the constant SFR and so on. The following yields were considered: $m_{Ia} = 0.6$, $m_{II} = 0.07$, and $m_{Ib} = 0.2$ except for OMS for which were taken 0.6, 0.05, 0.0, the second yield prescription, respectively. The different $m_{I,s}$ represent the masses ejected per each type of supernovae. In figure 2a we have plotted the age-metallicity relations along with the observational data from Twarog (1980) and in figure 2b the same age-metallicity relations but now along with the data from Carlberg et al. (1985), revised evaluation of Twarog's data. The relations have been normalized so that $[Fe/H]=0.0$ when the solar system was formed, at 4.6 billion years ago.

Fig. 3a-b Theoretical predictions of the $[Fe/O]$ - $[O/H]$ relationships. We have plotted six curves coming from the different star formation rate prescriptions for the second yield prescription. In figure 3b we have just plotted OMS in a more suggestive scale. The data are taken from Barbuy (1988) (squares) and from Nissen et al. (1985) (triangles).

Fig. 4a-c Theoretical predictions of the Mg, Si, and Ti abundances for OMS with the second yield prescription. The data are taken from Gratton and Sneden (GS, 1987), open squares, GS (1988), \times symbols, Hartmann and Gehren (1988), four pointed stars, and Magain (1989), solid squares.

Fig. 5a-b The evolution of the luminosity in bolometric magnitude units and normalized to the actual one, both with respect to age (a) and redshift (b), for different star formation rates.

Fig. 6a-b The number counts of galaxies in the B_J (a) and in the K band (b). The data are from Maddox et al. (1990), solid triangles, Metcalfe et al. (1991), solid squares, and Lilly et al. (1991) for the B_J band and from Cowie et al. (1992) for the K band. In both figures the solid line represents the non-evolutionary case.

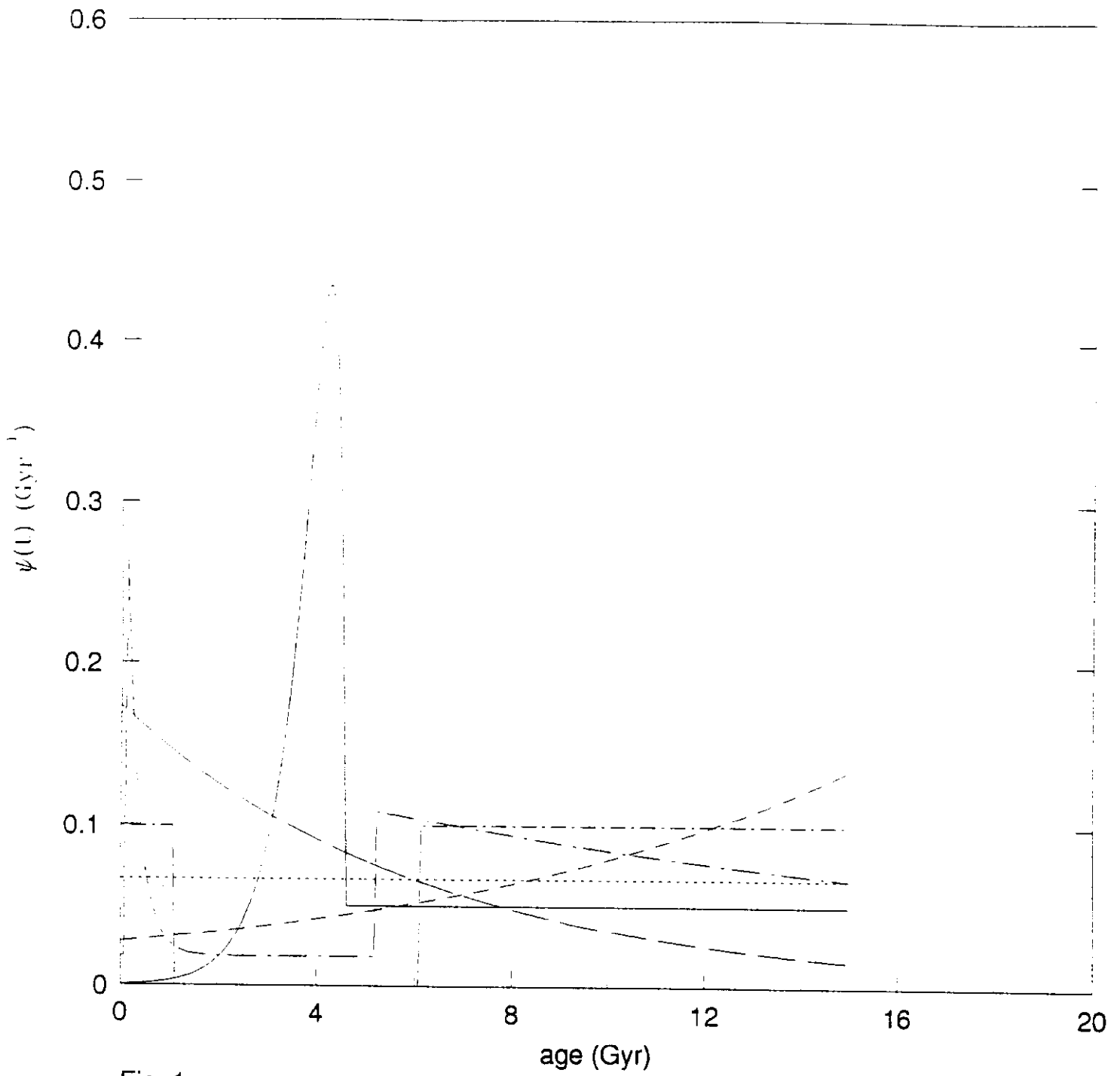


Fig. 1

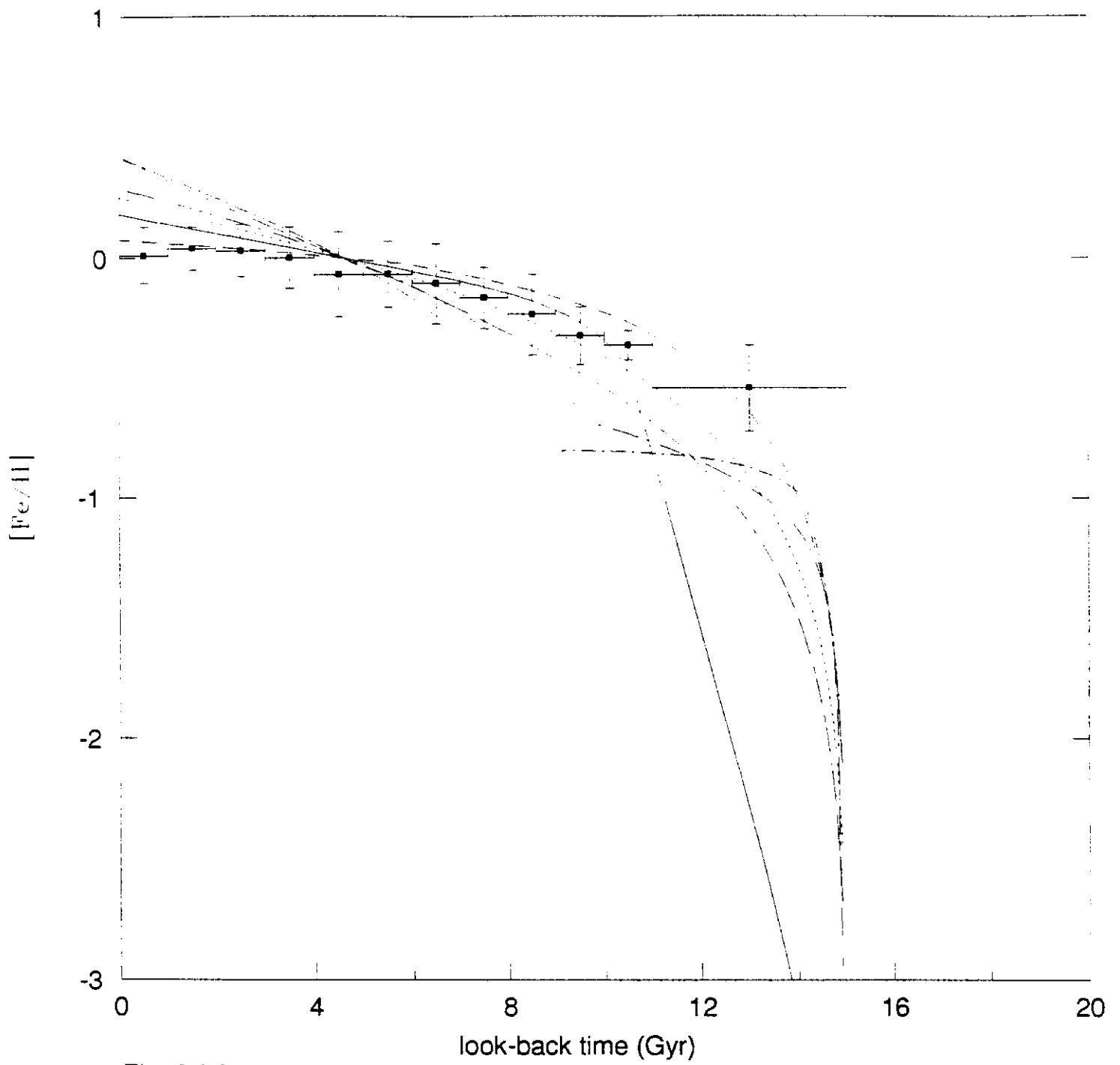


Fig. 2 (a)

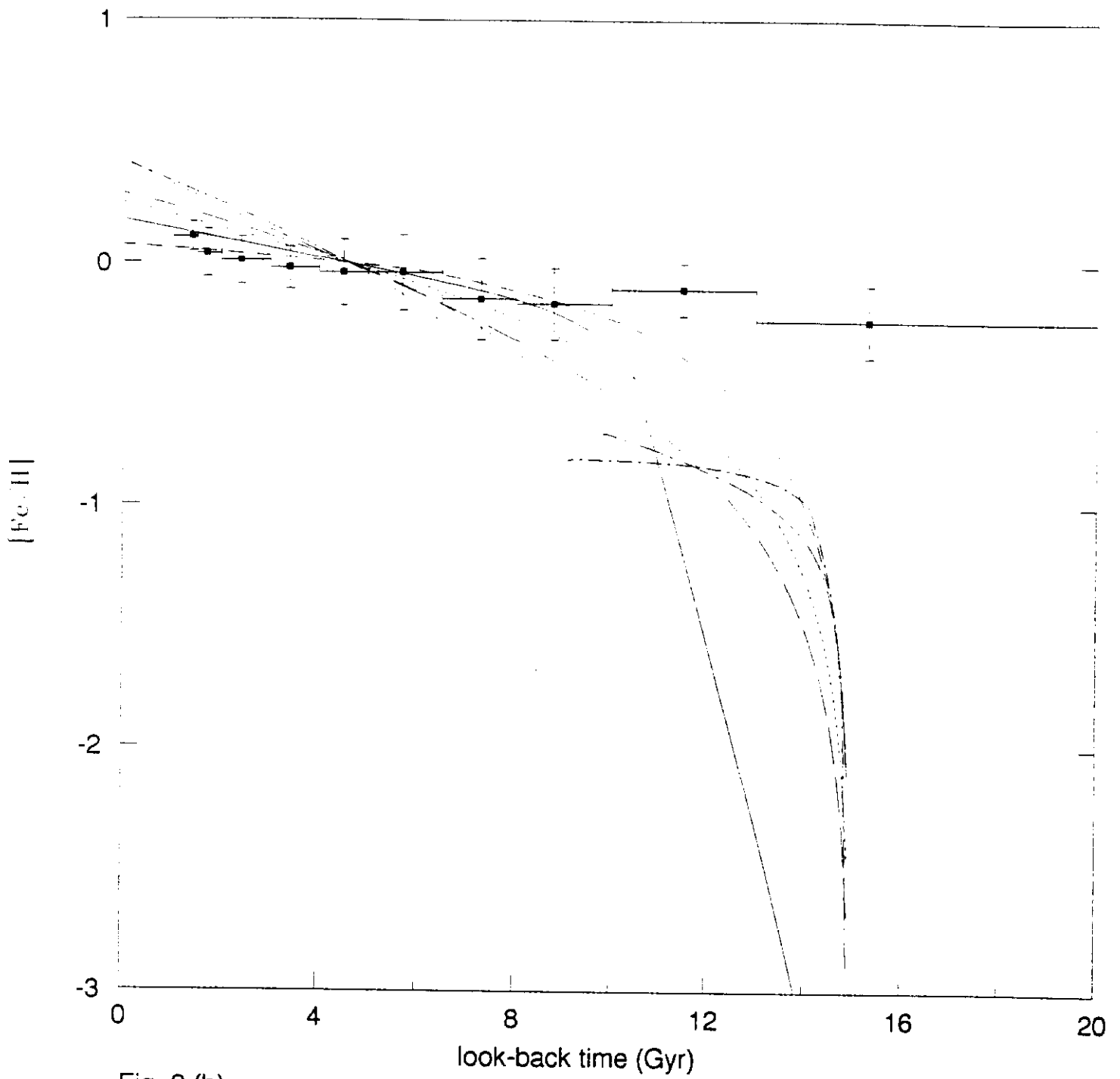


Fig. 2 (b)

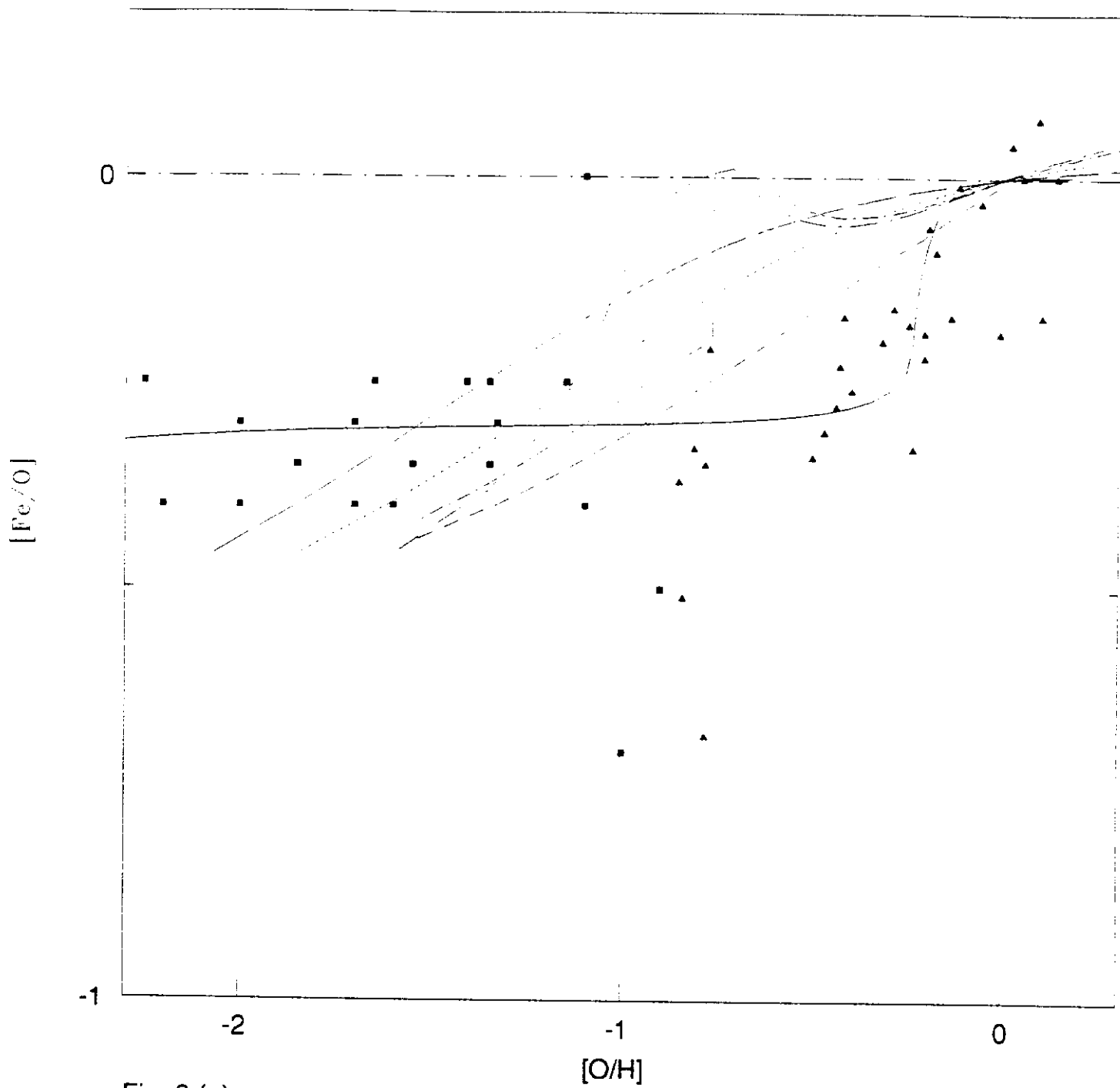


Fig. 3 (a)

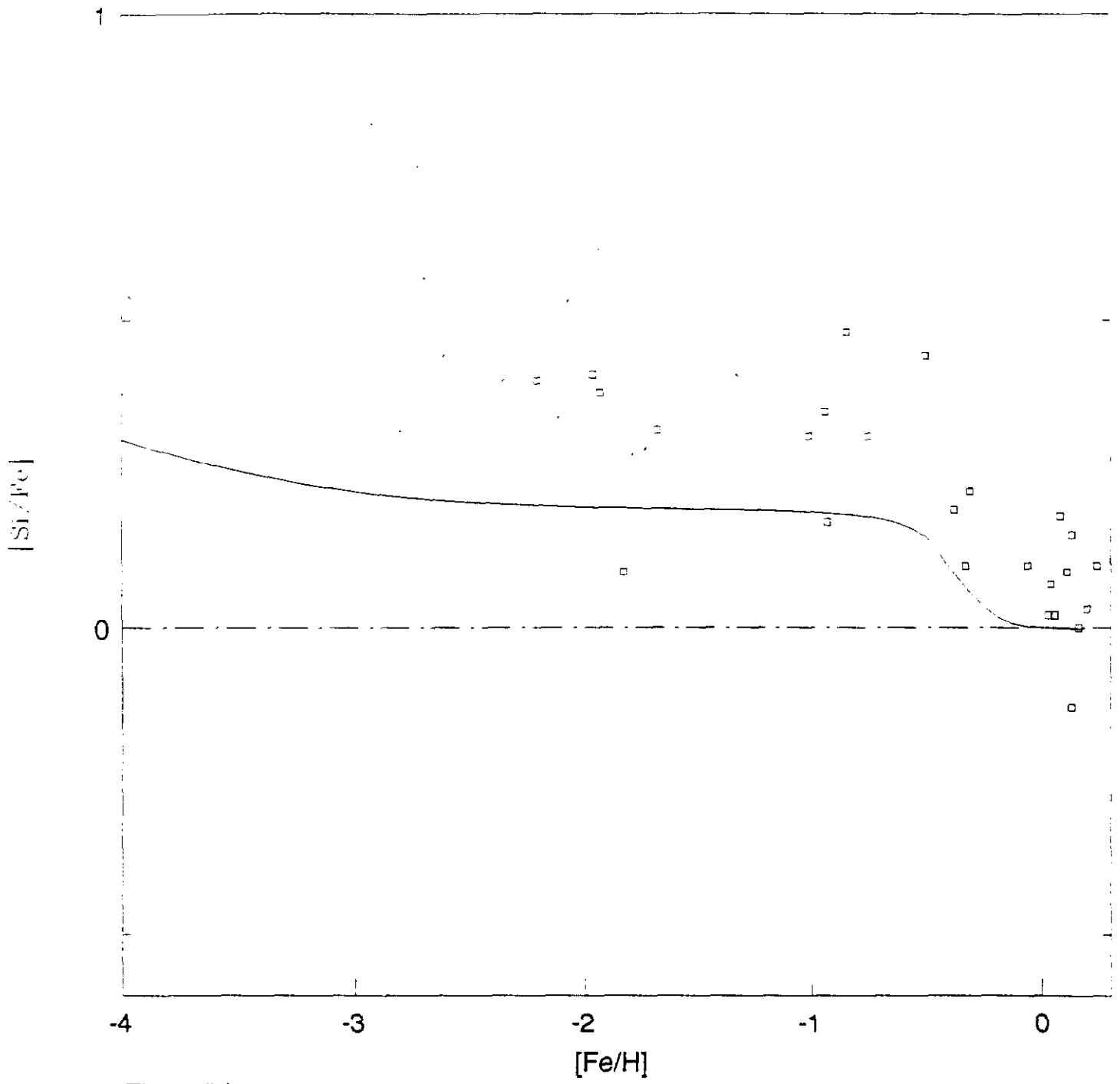


Fig. 4 (b)

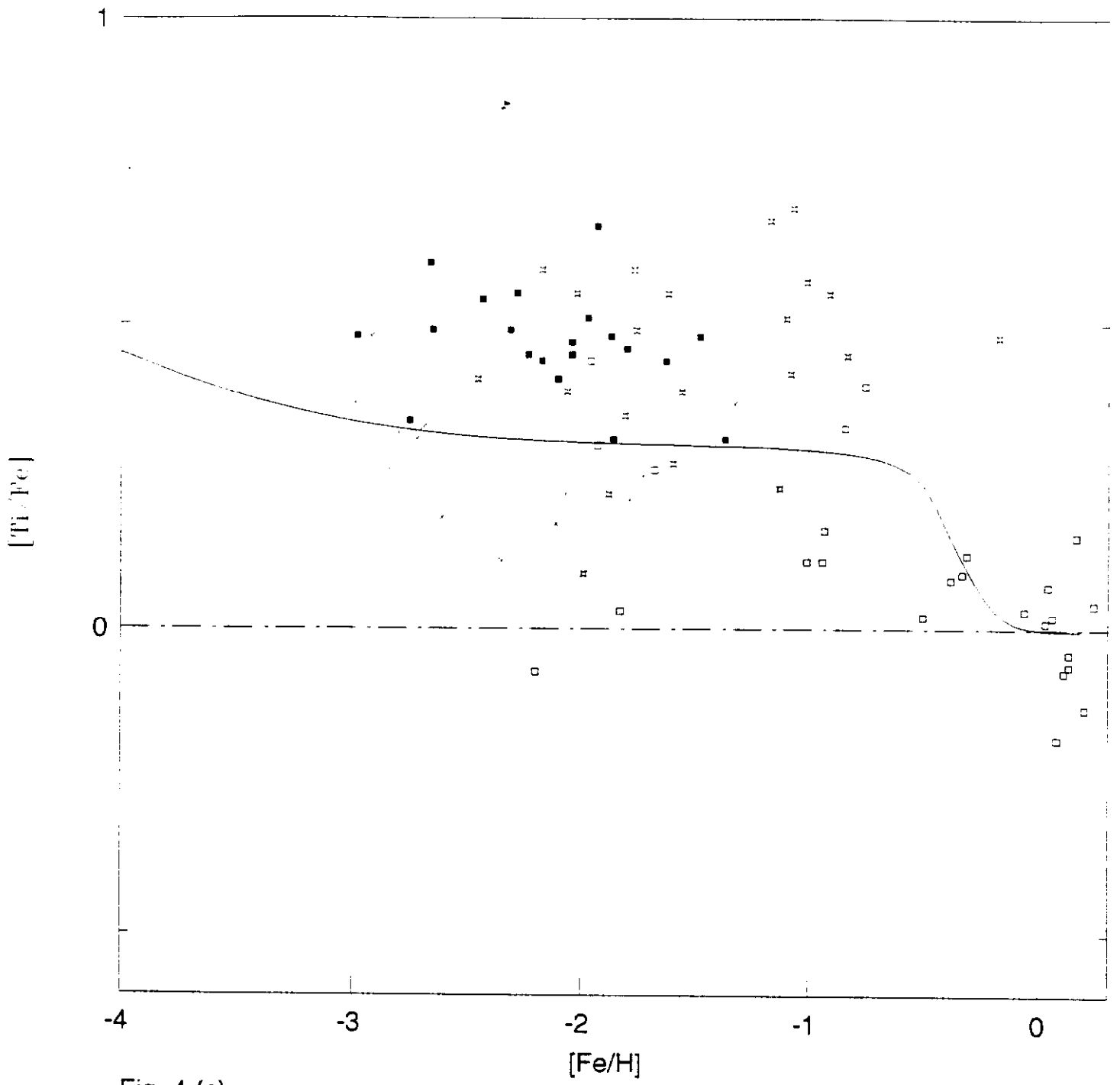


Fig. 4 (c)

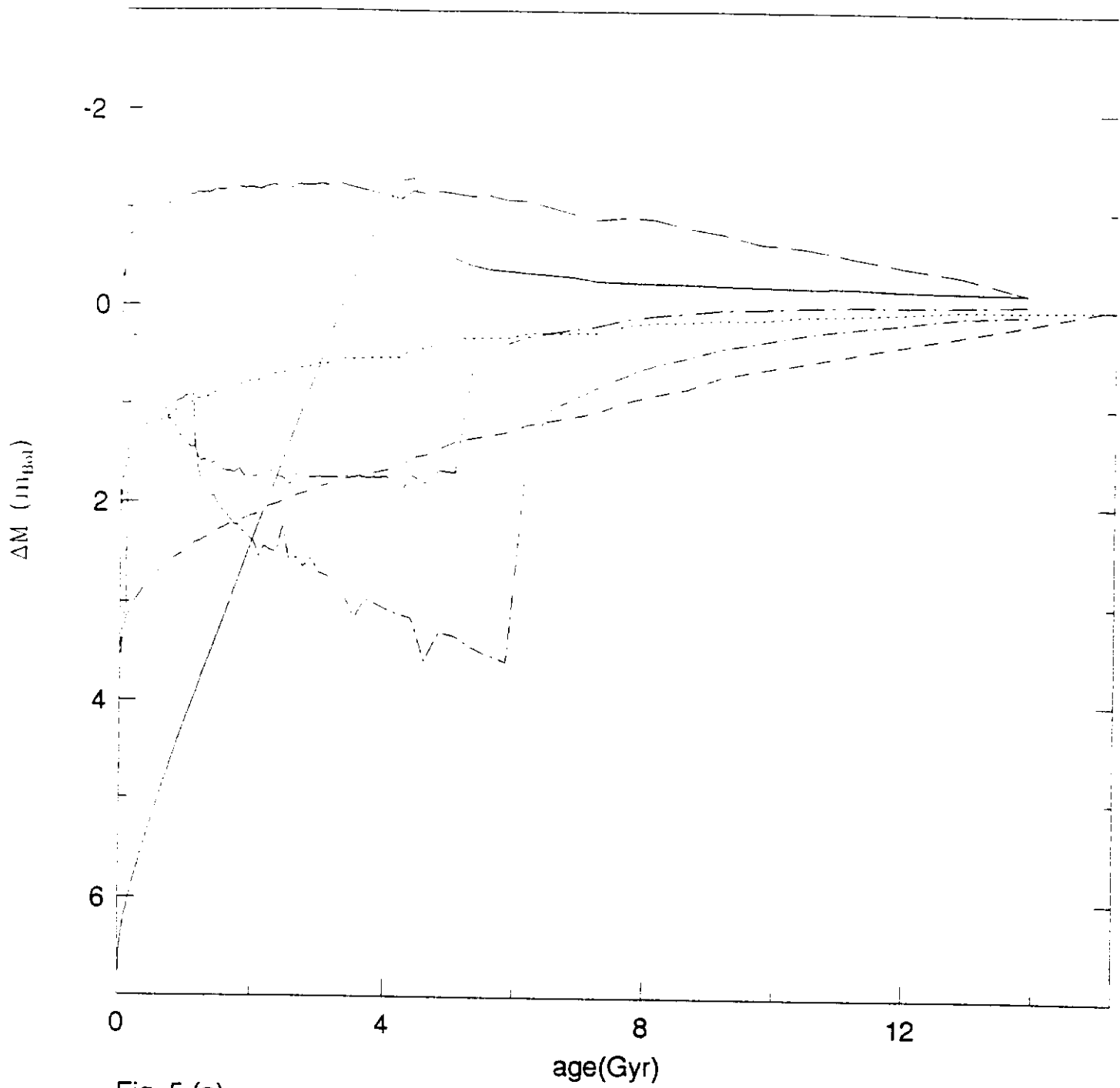


Fig. 5 (a)

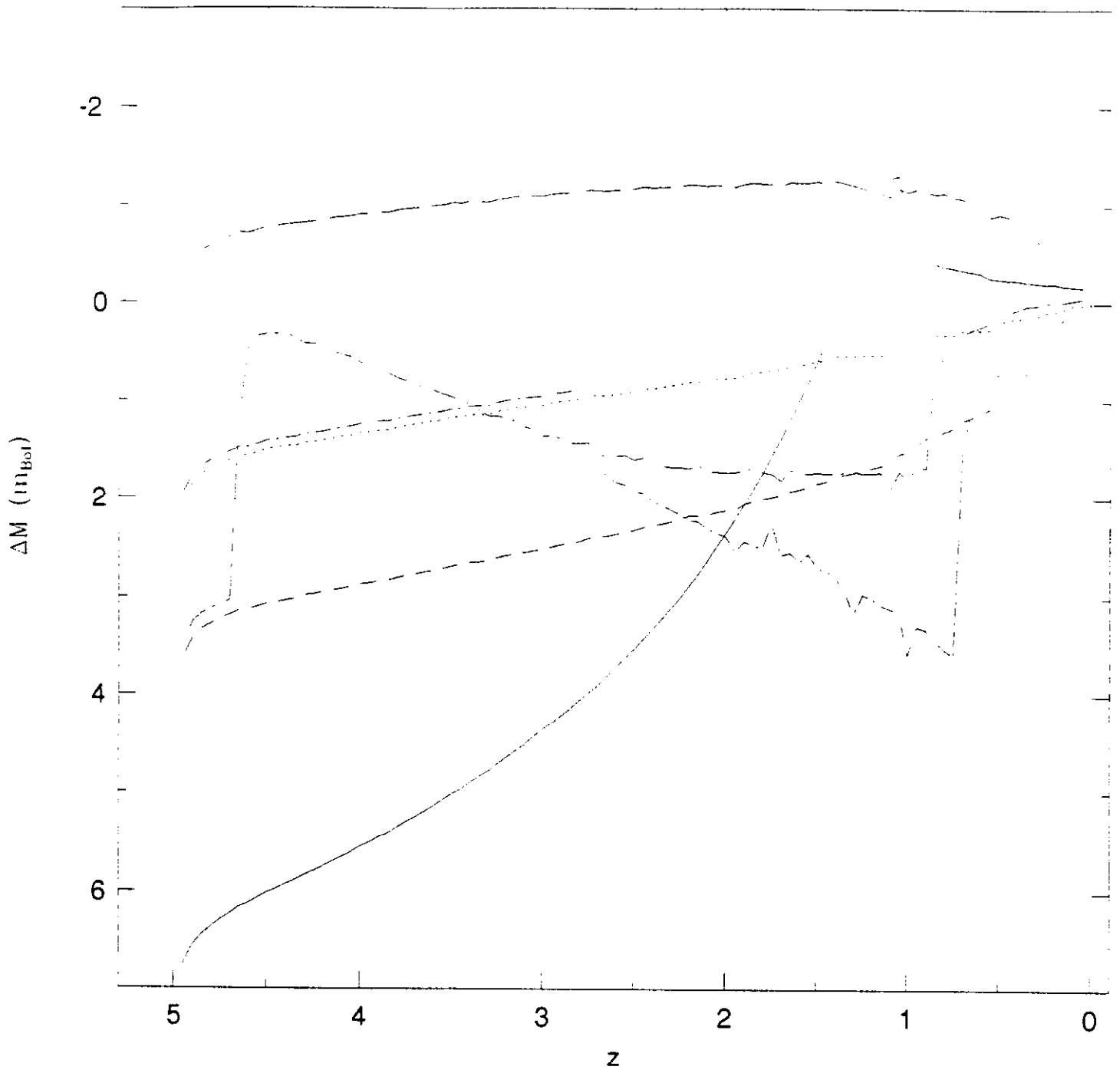


Fig. 5 (b)

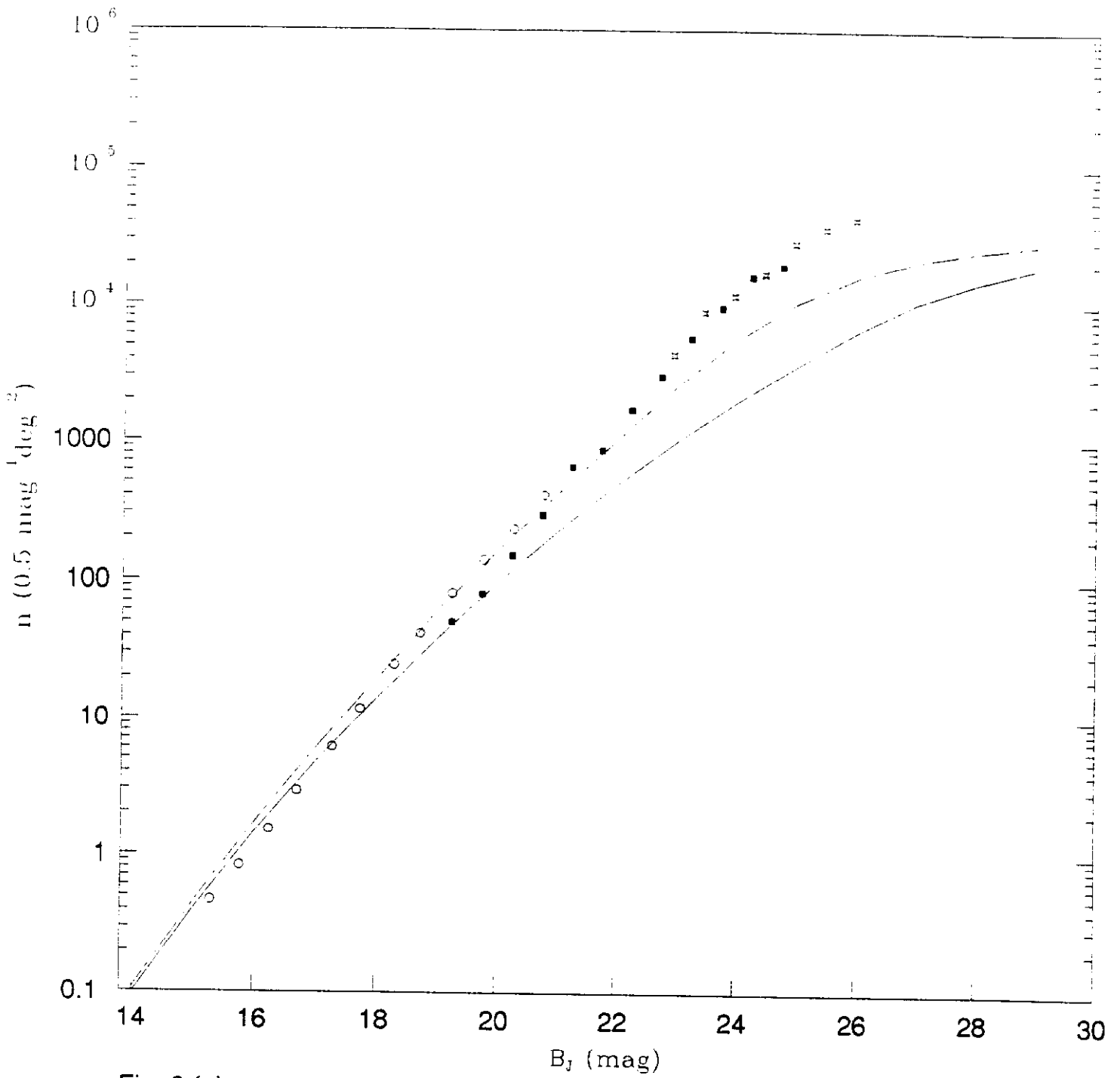


Fig. 6 (a)

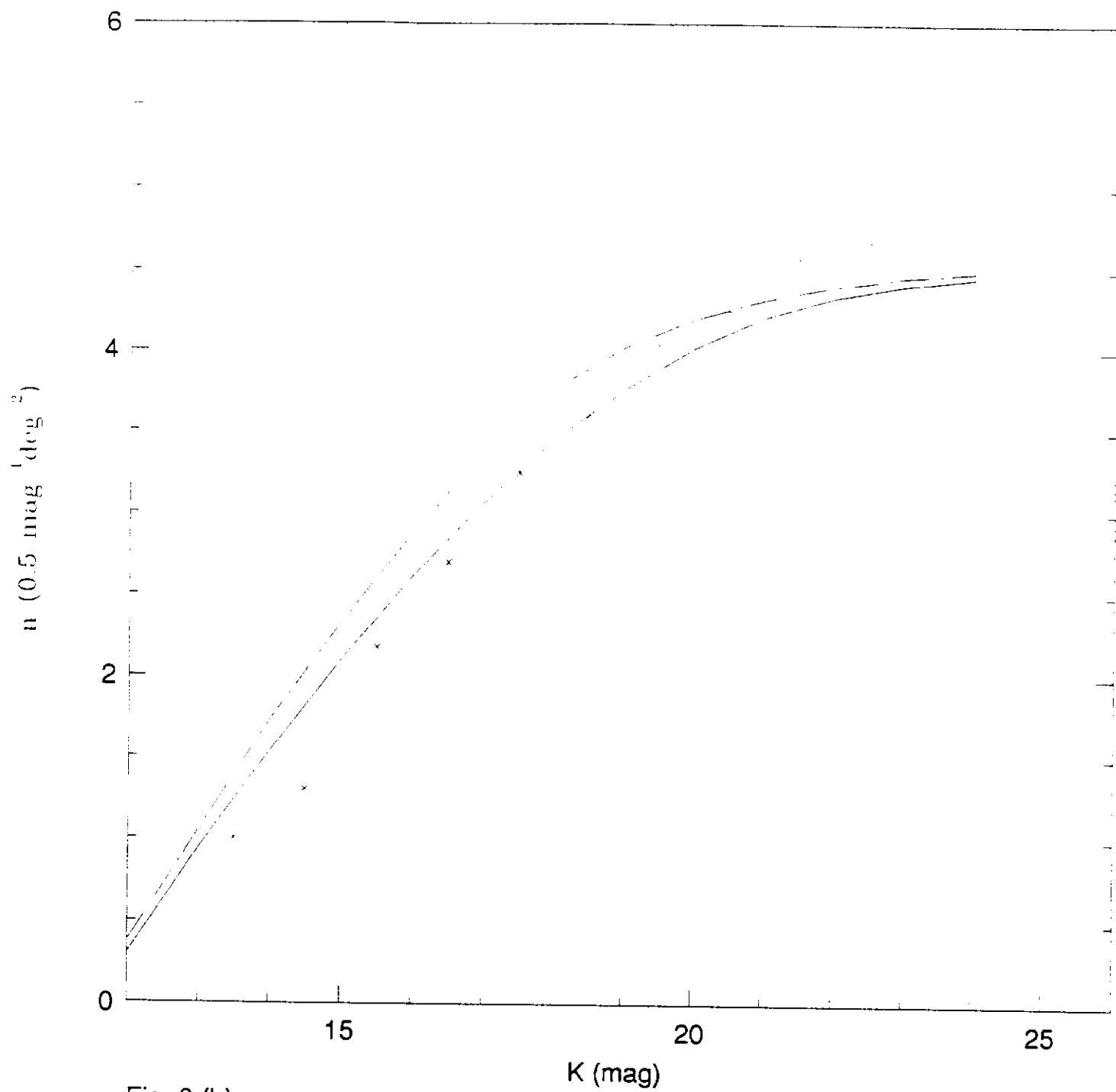


Fig. 6 (b)